



cDNA library screening identifies protein interactors potentially involved in non-telomeric roles of *Arabidopsis* telomerase

Ladislav Dokládal^{1,2}, David Honys³, Rajiv Rana³, Lan-Ying Lee⁴, Stanton Gelvin⁴ and Eva Sýkorová^{1,2*}

¹ Mendel Centre for Plant Genomics and Proteomics, Central European Institute of Technology and Faculty of Science, Masaryk University, Brno, Czech Republic, ² Institute of Biophysics – Academy of Sciences of the Czech Republic v.v.i., Brno, Czech Republic, ³ Institute of Experimental Botany – Academy of Sciences of the Czech Republic v.v.i., Prague, Czech Republic, ⁴ Department of Biological Sciences, Purdue University, West Lafayette, IN, USA

OPEN ACCESS

Edited by:

Inna Lermontova,
Institute of Plant Genetics and Crop
Plant Research, Germany

Reviewed by:

Biswapriya Biswas Misra,
University of Florida, USA
Chee How Teo,
Taylor's University, Malaysia

*Correspondence:

Eva Sýkorová
evin@ibp.cz

Specialty section:

This article was submitted to
Plant Cell Biology,
a section of the journal
Frontiers in Plant Science

Received: 02 September 2015

Accepted: 27 October 2015

Published: xx November 2015

Citation:

Dokládal L, Honys D, Rana R, Lee L-Y, Gelvin S and Sýkorová E (2015) cDNA library screening identifies protein interactors potentially involved in non-telomeric roles of *Arabidopsis* telomerase. *Front. Plant Sci.* 6:985. doi: 10.3389/fpls.2015.00985

Telomerase-reverse transcriptase (TERT) plays an essential catalytic role in maintaining telomeres. However, in animal systems telomerase plays additional non-telomeric functional roles. We previously screened an *Arabidopsis* cDNA library for proteins that interact with the C-terminal extension (CTE) TERT domain and identified a nuclear-localized protein that contains a RNA recognition motif (RRM). This RRM-protein forms homodimers in both plants and yeast. Mutation of the gene encoding the RRM-protein had no detectable effect on plant growth and development, nor did it affect telomerase activity or telomere length *in vivo*, suggesting a non-telomeric role for TERT/RRM-protein complexes. The gene encoding the RRM-protein is highly expressed in leaf and reproductive tissues. We further screened an *Arabidopsis* cDNA library for proteins that interact with the RRM-protein and identified five interactors. These proteins are involved in numerous non-telomere-associated cellular activities. In plants, the RRM-protein, both alone and in a complex with its interactors, localizes to nuclear speckles. Transcriptional analyses in wild-type and *rrm* mutant plants, as well as transcriptional co-analyses, suggest that TERT, the RRM-protein, and the RRM-protein interactors may play important roles in non-telomeric cellular functions.

Keywords: telomerase, nuclear poly(A)-binding protein, telobox, metallothionein 2A, MODIFIER OF *snc1*, putative nuclear DNA-binding protein G2p, oxidation-related zinc finger 2 protein, BiFC

INTRODUCTION

Telomeres are nucleoprotein structures at the ends of eukaryotic chromosomes, distinguishing these ends from double strand DNA breaks (DSBs) and protecting them from the DNA damage repair (DDR) machinery. Due to the “end replication problem” (Olovnikov, 1971; Watson, 1972; Olovnikov, 1973) telomeres are shortened in each round of replication until they are too short to function, leading to cell senescence (Levy et al., 1992) and apoptosis (Harley et al., 1990; Counter et al., 1992). Thus, telomeres limit cellular proliferative capacity and act as a biological “clock.” On the other hand, in cells with high proliferative need such as animal embryonic, stem, and cancer cells (reviewed in Blasco, 2005), or plant meristemic cells (Fitzgerald et al., 1996), telomere shortening is compensated by the action of telomerase, a conserved ribonucleoprotein complex

with a reverse transcriptase subunit (Greider and Blackburn, 1985, 1987). Telomerase consists of two core subunits, telomerase RNA (TR) and telomerase reverse transcriptase (TERT), that are associated with several additional proteins not crucial for enzymatic activity. The TERT subunit has an evolutionary conserved primary structure which in most organisms can be further divided into N-terminal domains TEN (telomerase essential N-terminal) and TRBD (TR binding domain), a central reverse transcriptase (RT) domain, and a C-terminal extension (CTE; reviewed in Sykorova and Fajkus, 2009).

The fact that telomerase influences cellular life span and plays a role in various types of cancer intensified research in this field. Surprisingly, telomerase in mammalian cells influences tumorigenesis by additional mechanisms independent of telomere synthesis (reviewed in Majerska et al., 2011). These so-called non-telomeric functions of telomerase regulate processes such as apoptosis, cellular proliferation, and cell cycle regulation, generally by altering gene expression, or DDR by *de novo* telomere addition to the sites of DDB.

For the above reasons it is of great interest to study mechanisms and interactions through which telomerase is regulated, and by which telomerase regulates cellular functions other than telomere synthesis.

Telomerase from *Arabidopsis thaliana* represents a suitable model, especially because of the availability of viable T-DNA insertion mutants that are typically exploited in these types of studies. Classically, changes in telomere length and telomerase activity are measured in a particular mutant, which may lead to direct identification of important telomerase regulators. However, this approach may not detect interactors crucial for mediating non-telomeric activities of telomerase. For this purpose, methods such as tandem affinity purification or cDNA library screening may be more suitable.

The N- and C-terminal portions of TERT represent potential interacting targets for telomerase regulatory proteins. The CTE is highly conserved among vertebrates and plants and contains regions important for intracellular trafficking of human TERT, including a nuclear export signal, 14-3-3, and CRM1 binding sites (Seimiya et al., 2000). In our previous work we screened for *Arabidopsis* CTE protein–protein interactions against a cYFP-tagged *Arabidopsis* cDNA library in tobacco BY-2 protoplasts and identified two interacting partners, an armadillo/ β -catenin-like repeat containing protein (encoded by At4g33945) interacting with CTE in the cytoplasm, and an RRM-containing protein (encoded by At5g10350; RRM) that interacts with the CTE in nuclei (Lee et al., 2012).

How telomerase executes its non-canonical activities and on which levels it regulates expression of its target genes are poorly understood. One possibility is regulation on the level of mRNA. The RRM protein belongs to a subfamily of *Arabidopsis* nuclear poly(A) binding proteins; that are characterized by a single RRM domain close to the C-terminus (reviewed in Eliseeva et al., 2013). The human nuclear poly(A) binding protein PABPN1 is implicated in a variety of mRNA stabilization and degradation processes, such as stimulation of poly(A) synthesis by poly(A) polymerase, protection of growing poly(A) chains from degradation, defining the length of growing poly(A) chains,

and mRNA export (Wahle and Ruegsegger, 1999; Keller et al., 2000; Kuhn et al., 2009). In addition to RNA binding, the RRM domain may be responsible for interactions with other proteins or DNA (reviewed in Krietsch et al., 2013). These observations support the hypothesis that the interaction between TERT and RRM might be a mechanism by which telomerase could affect many cellular processes.

Here, we present further characterization of the RRM protein and discuss its potential physiological role in telomerase involvement in non-telomeric activities. We describe the interaction profile of the RRM protein and analyze telomere length, telomerase activity, and changes in gene expression in T-DNA insertion mutants that disrupt the *RRM* gene.

MATERIALS AND METHODS

Plant Material

Arabidopsis T-DNA insertion lines SALK_096285 (*rrm-1*) and SALK_116646C (*rrm-2*) were obtained from the Nottingham *Arabidopsis* Stock Centre. Both mutant and wild type (Col-0) *A. thaliana* seeds were surface sterilized and germinated on 0.8% (w/v) agar plates supplemented with 1/2 Murashige and Skoog media (MS; cat. n. M0255.0050; Duchefa¹) and 1% (w/v) sucrose. Seedlings were potted after 7 days and further grown in the conditions of 16 h light, 21°C and 8 h dark, 19°C, illumination 150 $\mu\text{mol m}^{-2} \text{s}^{-1}$. Individual plants from each T-DNA insertion line were genotyped (see Supplementary Table S1 for primer sequences) and after selection of homozygous mutant plants, three subsequent generations were grown.

Telomere Length and Telomerase Activity Analyses

The terminal restriction fragment (TRF) analysis using Southern blot hybridization, the conventional TRAP (telomere-repeat-amplification-protocol) and the quantitative TRAP assays were performed as described (Fojtová et al., 2011). Mean telomere length values were calculated using TeloTool software (Gohring et al., 2014).

Entry Clone Generation

Sequences encoding full-length RRM (At5g10350) and G2p (At3g51800) proteins were amplified from 7-days-old seedling cDNA by Phusion HF DNA polymerase (Finnzymes²) according to the manufacturer's instructions. Sequences encoding RRM fragments [RRM-1(1–81); RRM-2(1–169); RRM-3(170–217); RRM-4(82–217); RRM-5(82–169)] were sub-cloned using KAPA Taq DNA polymerase (Kapabiosystems³) and a pGADT7-DEST::RRM construct as a template. Primers used for cloning are listed in Supplementary Table S1. PCR products were precipitated using PEG and cloned into pDONR/Zeo (Invitrogen⁴). The MT2A (At3g09390) coding sequence was sub-cloned into

¹<https://www.duchefa-biochemie.com/>

²<http://www.thermoscientificbio.com/finnzymes>

³www.kapabiosystems.com

⁴<http://www.lifetechnologies.com>

229 pDONR/zeo from the cYFP cDNA library clone 212M1
 230 (Lee et al., 2012). Entry clones encoding HSP70-1 (stock
 231 no. GC104920, At5g02500) and OZF2 (stock no. G10332,
 232 At4g29190; Kayoko et al., 2003) were obtained from the
 233 ABRC⁵. Entry clones encoding AtTERT (At5g16850) fragments
 234 TEN(1–233), RID1(1–271), Fw3N-NLS(229–582), RT(597–987),
 235 and CTE2(958–1123) were prepared previously (Zachova et al.,
 236 2013).

237 Yeast Two Hybrid Analysis

238 Yeast two-hybrid experiments were performed using the
 239 MatchmakerTM GAL4-based two-hybrid system (Clontech⁶).
 240 cDNA sequences encoding RRM protein (full-length and
 241 fragments), TERT fragments, G2p, MT2A, HSP70-1, and OZF2
 242 were subcloned from their entry clones into the destination
 243 vectors pGADT7-DEST and pGBKT7-DEST. Each bait/prey
 244 combination was co-transformed into *Saccharomyces cerevisiae*
 245 PJ69-4a and yeast two hybrid analysis was performed as described
 246 in Schruppová et al. (2014). Protein expression was verified
 247 by immunoblotting using mouse anti-HA (kindly provided
 248 by Dr. Vojtěšek) or mouse anti-myc primary antibodies and
 249 HRP-conjugated anti-mouse secondary antibody (both Sigma-
 250 Aldrich⁷).

251 Bimolecular Fluorescence 252 Complementation and Screening of 253 cYFP cDNA Library

254 The constructs nYFP-TERT(CTE2), n/cYFP-TERT(RID1),
 255 and cYFP-RRM were created previously (Lee et al., 2012;
 256 Schruppová et al., 2014). The RRM, G2p, HSP70-1, and
 257 OZF2 coding sequences were subcloned from their entry clones
 258 into the destination vector pSAT4-DEST-nEYFP-C1 (Gelvin
 259 laboratory stock number pE3136). To visualize RRM subcellular
 260 localization, the RRM coding sequence was subcloned into
 261 the destination vector p2YGW7, generating a YFP tag at the
 262 N-terminus of the protein. The nYFP-RRM construct was
 263 screened against a cYFP cDNA library for protein-protein
 264 interactions in tobacco BY-2 protoplasts as described (Lee et al.,
 265 2012).

266 Tobacco BY-2 protoplasts were isolated and transfected as
 267 previously described (Tenea et al., 2009; Lee et al., 2012).
 268 *Arabidopsis* leaf protoplasts were isolated and transfected as
 269 described by Wu et al. (2009). To label cell nuclei, we co-
 270 transfected a plasmid expressing mRFP fused to the nuclear
 271 localization signal of the VirD2 protein from *Agrobacterium*
 272 *tumefaciens* (mRFP-VirD2NLS; Citovsky et al., 2006). To
 273 label nuclear speckles, a pSRp30-RFP nuclear speckles marker
 274 (Lorkovic et al., 2004) was co-transfected. Transfected protoplasts
 275 were incubated in the dark at room temperature overnight,
 276 and observed for fluorescence using a Zeiss AxioImager Z1
 277 epifluorescence microscope (Tobacco BY-2) or a Leica SPE
 278 confocal scanning light microscope (*Arabidopsis*). As a negative
 279 control, we used the constructs nYFP- and cYFP-GAUT10

280 (At2g20810). Protein expression was tested by immunoblotting
 281 using mouse anti-GFP primary antibody (Roche⁸) and HRP-
 282 conjugated anti-mouse secondary antibody (Sigma-Aldrich).
 283 Proteins were extracted from protoplasts into an extraction buffer
 284 (50 mM Na₂HPO₄, 10 mM EDTA, 0.1% Triton X-100, 10 mM 2-
 285 Mercaptoethanol, 1x Proteinase inhibitors cocktail, 1 mM PMSF)
 286 by vortexing.

287 RNA Isolation and RT-qPCR Analysis

288 RNA from various *Arabidopsis* pollen developmental stages
 289 (Hony and Twell, 2004) was isolated using a Plant RNeasy
 290 Kit (Qiagen⁹) according to the manufacturer's instructions, and
 291 further purified by DNaseI treatment (TURBO DNA-free kit,
 292 Thermo Fisher Scientific¹⁰). RNA isolation from other tissues
 293 of mutant or wild-type plants and reverse transcription were
 294 performed as described (Fojtová et al., 2011; Ogrocka et al.,
 295 2012). Calli were derived from 7-days-old seedlings, propagated
 296 on cultivation medium with 1 μg ml⁻¹ 1-naphthaleneacetic acid
 297 and 1 μg ml⁻¹ 2,4-dichlorophenoxyacetic acid, and subcultured
 298 monthly onto fresh medium. Transcript levels relative to a
 299 ubiquitin reference gene were analyzed using FastStart SYBR
 300 Green Master (Roche) and a 7300 Real-Time PCR System
 301 (Applied Biosystems¹¹). A 1 μl aliquot of cDNA was added to the
 302 20 μl reaction mix; the final concentration of each forward and
 303 reverse primer (Supplementary Table S1) was 0.5 μM. Reactions
 304 were performed in triplicate; PCR cycle conditions consisted of
 305 10 min of initial denaturation followed by 40 cycles of 20 s at
 306 95°C, 30 s at 55°C, and 1 min at 72°C. SYBR Green I fluorescence
 307 was monitored after each extension step. The amount of the
 308 respective transcript was determined for at least two biological
 309 replicates using the ΔΔCt method (Pfaffl, 2004).

310 Identification of Genes Co-regulated 311 with RRM

312 GENEVESTIGATOR (Nebion AG¹²) application (Hruz et al.,
 313 2008) was used to identify *in silico* genes co-regulated with
 314 RRM and genes encoding its interacting partners TERT,
 315 G2P, MOS1, OZF2, HSP70-1, and MT2A. Using this tool,
 316 we first defined conditions under which any of these genes
 317 shows an at least twofold change in transcript levels. We
 318 then searched for genes responding either in a similar
 319 (score 0 to 1) or opposite (score -1 to 0) manner on
 320 the same subset of defined conditions. Genes with a co-
 321 regulation level score either higher than 0.5 or lower than
 322 -0.5 were considered for further analyses. Telobox motifs in
 323 candidate genes were identified in the literature or by manually
 324 searching for the motifs AAACCCT, AACCCCTA and their
 325 corresponding reverse complements, in the genomic region
 326 1000 bp upstream of the translation start (ATG) site using

327 ⁸www.roche.com

328 ⁹www.qiagen.com

329 ¹⁰www.thermofisher.com

330 ¹¹www.appliedbiosystems.com

331 ¹²https://genevestigator.com/gv/

332 ⁵http://www.arabidopsis.org/

333 ⁶www.clontech.com

334 ⁷www.sigmaaldrich.com

publically available data at NCBI¹³ and/or the gene datasets from Wang et al. (2011). Putative protein–protein-interaction networks were visualized using STRINGv10¹⁴ (Szklarczyk et al., 2015).

RESULTS

Verification of *In vivo* Interaction between the RRM Protein and the CTE Domain of AtTERT

The RRM protein was identified as a putative interaction partner of AtTERT by screening a cYFP-tagged cDNA library using BiFC in tobacco BY-2 protoplasts (Lee et al., 2012). To test if this interaction is independent of the plant system used, we expressed both tagged partners in *Arabidopsis* leaf protoplasts and observed a positive BiFC signal in the nucleus (Figure 1A). We further employed the yeast-two-hybrid (Y2H) system, but no interaction was observed in yeast despite the expression of both proteins (Supplementary Figure S1). These results suggested that the *in vivo* interaction between the RRM and the AtTERT CTE domain was mediated by an additional plant protein or protein modification absent in yeast cells but present in telomerase-positive (BY-2) and telomerase-negative (*Arabidopsis* leaf) cells.

The C-terminus of the RRM Protein is Responsible for RRM Dimerization

We tested the ability of the At5g10350 protein containing a single RRM domain to form homodimers using Y2H and BiFC analyses (Figures 1B,C). RRM dimerization was observed using BiFC in tobacco BY-2 protoplasts, where the interaction provided a pattern similar to that of full length RRM-YFP fusion protein that co-localized with the pSRp30-RFP nuclear speckles marker (Figure 1B). We further tested this interaction using Y2H where the RRM protein showed strong self-interaction using both histidine and stringent adenine growth selection (Figure 1C). To determine which part of the RRM molecule is responsible for dimerization, we prepared five constructs corresponding to various structural domains of the RRM protein. We tested them for interaction with full length RRM and with each other (Figure 1C) by Y2H analysis. The RRM-4(82–217) fragment comprising the RRM domain and the C-terminus, and the RRM-3(170–217) fragment with the C-terminus only, interacted with the full length RRM protein, each other, and themselves using both histidine and stringent adenine growth selection, suggesting that the C-terminus is responsible for protein homodimerization. The fragments RRM-1(1–81) – N-terminus, RRM-2(1–169) – N-terminus, and RRM-5(82–169) did not show positive Y2H signals, although their successful expression was confirmed by immunoblotting (Supplementary Figure S1).

¹³<http://www.ncbi.nlm.nih.gov/>

¹⁴<http://www.string-db.org/>

BiFC Screening of an *Arabidopsis* cDNA Library Identified Proteins that Interact with the RRM Protein

To obtain better insights into possible RRM cellular functions and its involvement in specific cellular processes, we screened in BY-2 protoplasts a nYFP-RRM fusion protein against a cYFP cDNA library (Lee et al., 2012). We identified one cDNA clone encoding the full length protein Metallothionein 2A protein (At3g09390; MT2A) and four additional cDNA clones encoding protein fragments that were in-frame with the YFP tag (Figure 2): (i) Modifier Of Snc1 (MOS1; At4g24680; fragment 1040–1427 aa); (ii) the putative nuclear DNA-binding protein G2p (At3g51800; 347–401 aa); (iii) Oxidation Related Zinc Finger 2 (OZF2; At4g29190; 1–68 aa); (iv) Heat Shock Cognate protein 70-1 (HSP70-1; At5g02500; 1–211 aa). In all cases, the interaction signal resembled nuclear speckles. We generated Y2H and BiFC constructs of G2p, OZF2, and HSP70-1 bearing the respective full length coding sequences to confirm interaction with the RRM protein and to test interaction with AtTERT fragments (Figure 2B). We were unable to obtain a full length MOS1 (1–1427 aa) construct, either by RT-PCR in our laboratory or from stock centers. Using the Y2H system we found strong interaction between OZF2 and RRM proteins, whereas MT2A, G2p, and HSP70-1 did not interact with RRM. None of the proteins interacted with any AtTERT fragments (not shown). Interestingly, using BiFC in tobacco BY-2 protoplasts we found interaction of the G2p and MT2A proteins with RRM and also with the N-terminal domain fragment RID1(1–271) of AtTERT (Figure 2, Supplementary Figure S2), with strong nucleolar and weak nucleoplasmic localization.

RRM is Highly Expressed in Leaves and Reproductive Tissues

To characterize RRM expression during plant development, we investigated the level of RRM transcripts (Figure 3A), including in telomerase-positive tissues. The transcripts were quantified in flower buds, calli, leaves, and 7-days-old seedlings of wild-type plants with a particular interest in detailed seedling analysis comprising whole seedlings, shoots, roots, and root tips. To quantify transcript levels in reproductive tissues, we included five pollen developmental stages (uninucleate microspores, early bicellular pollen, late bicellular pollen, immature tricellular pollen, and mature pollen). We observed RRM transcripts in all tissues tested. However, the greatest RRM transcript abundance was seen in proliferating tissues – young leaves and reproductive tissues. During pollen development, RRM transcript abundance peaked at the time of pollen mitosis I. Our RT-qPCR data confirmed previously published microarray data¹⁵.

Telomere Length and Telomerase Activity in Homozygous *rrm* T-DNA Insertion Lines

To examine the role of RRM *in planta*, we analyzed *Arabidopsis* lines SALK_096285 (*rrm-1*) and SALK_116646C (*rrm-2*)

¹⁵<http://bbc.botany.utoronto.ca/>

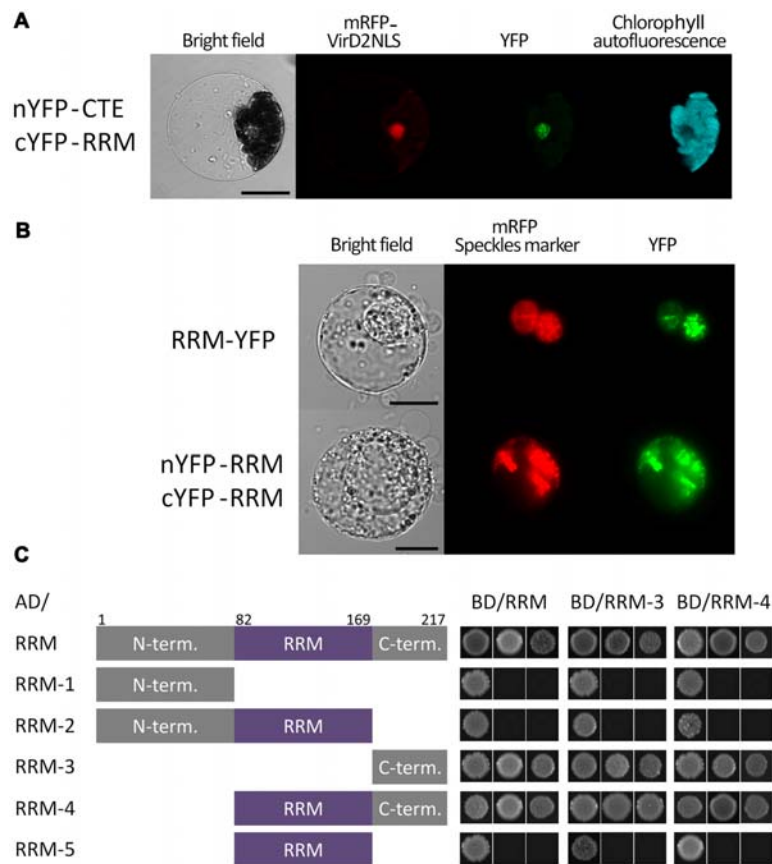


FIGURE 1 | Subcellular localization and dimerization of the RRM protein and verification of its interaction with the CTE domain of AtTERT. (A) BIFC in *Arabidopsis* leaf protoplasts confirmed a nuclear interaction of the RRM protein with AtTERT CTE domain. Protoplasts were co-transfected with plasmids encoding nYFP-tagged TERT(CTE2), cYFP-tagged RRM, and mRFP-VirD2(NLS) to label cell nuclei; nYFP- and cYFP-GAUT10 constructs served as negative control (not shown). YFP fluorescence is shown in green, mRFP fluorescence in red, and chlorophyll autofluorescence in blue pseudocolor. Scale bar indicates 10 μ m. **(B)** RRM-YFP co-localizes with a pSRp30-RFP nuclear speckle marker in tobacco BY-2 protoplasts. The same localization pattern was observed for interaction of nYFP-RRM with cYFP-RRM. YFP fluorescence is shown in green, and mRFP fluorescence of the VirD2(NLS) marker is shown in red. Scale bars indicate 20 μ m. **(C)** A Y2H system was used to assess RRM dimerization. Two sets of plasmids carrying full-length RRM or indicated RRM segments fused to either the GAL4 DNA-binding domain (BD) or the GAL4 activation domain (AD) were constructed and introduced into *Saccharomyces cerevisiae* PJ69-4a carrying *His3* and *Ade2* reporter genes. Co-transformation with an empty vector served as a negative control (not shown). Full-length RRM protein self-interacted on both histidine and stringent adenine selection plates. The same result was observed for interactions of the RRM-4(82–217) and the RRM-3(170–217) fragments with the full-length RRM protein, each other, and themselves, suggesting that the RRM-protein C-terminus is responsible for protein homodimerization. None of the other fragments [RRM-1(1–81), RRM-2(1–169), and RRM-5(82–169)] showed interaction, although their successful expression was confirmed by immunoblotting (Supplementary Figure S1).

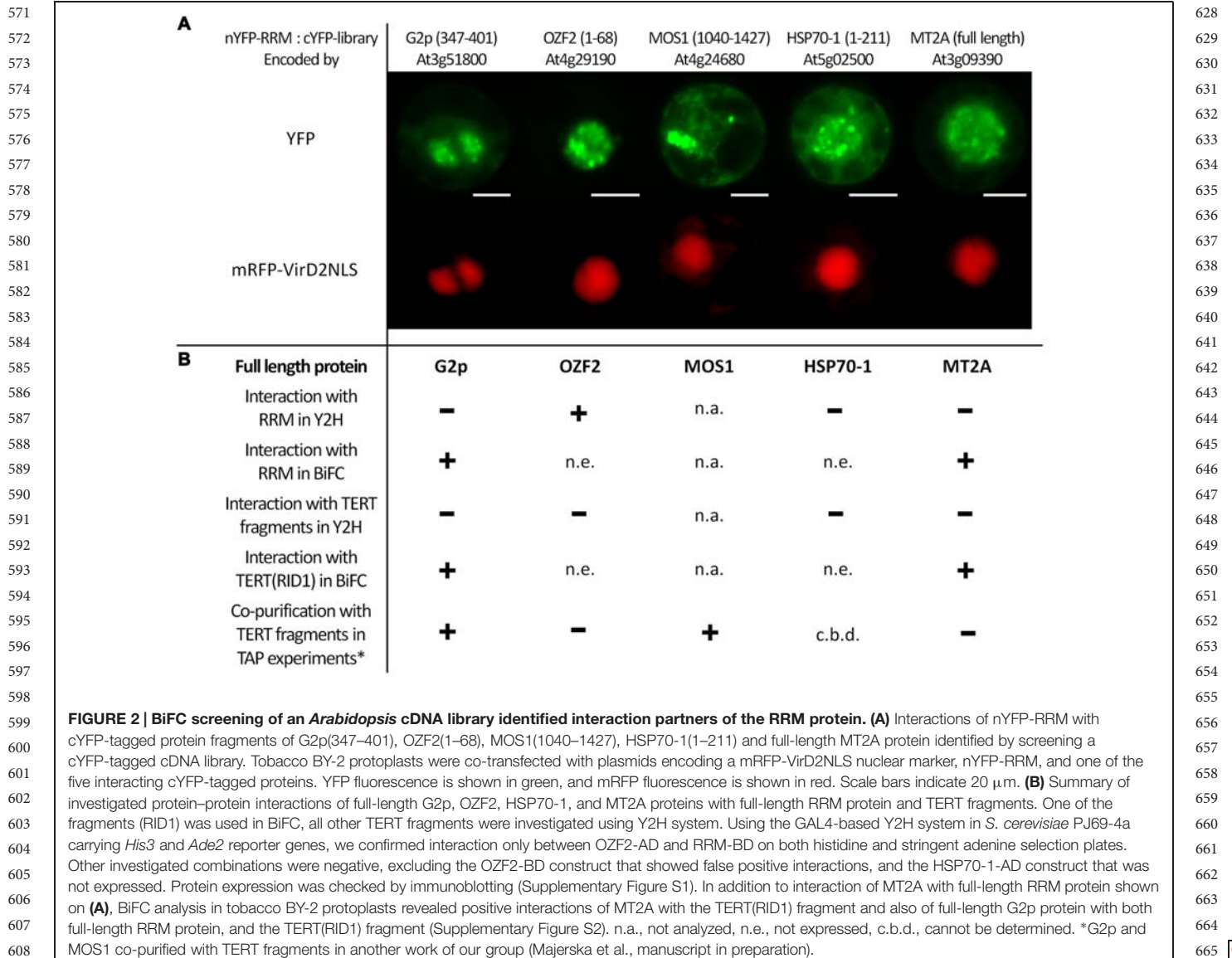
harboring different T-DNA insertions in the *RRM* gene (Figure 3B). RT-qPCR results confirmed only *rrm-1* as a null allele, whereas the *rrm-2* allele caused only a partial knock-down of the *RRM* transcript (Figure 3C). No detectable morphological differences were observed in root length, rosette diameter, leaf number, flowering time, or silique number comparing soil-grown wild-type (Col-0) and three subsequent generations of homozygous *rrm*^{-/-} plants (not shown). Thus, RRM function does not appear to be essential for plant growth and development under these experimental conditions.

Telomere length was determined in three independent homozygous G3 mutant plants using the TRF analysis. Although telomeres in both *rrm-1/rrm-1* and *rrm-2/rrm-2* G3 generation plants were slightly longer when compared to wild-type plants

(Supplementary Figure S3), a paired Student *t*-test indicated that these changes were not significant (the two-tailed *p*-values equal 0.0575 and 0.0656 for *rrm-1* and *rrm-2*, respectively). Telomerase activity in G3 generation homozygous *rrm-1* and *rrm-2* lines was tested by TRAP (telomere repeat amplification protocol) in 7-days-old seedlings. No changes in telomerase activity or processivity were observed using conventional TRAP analysis or quantitative TRAP analysis (not shown).

Changes in Transcripts Levels in Homozygous *rrm* Lines

We analyzed the transcription profiles of genes identified by our cDNA library screen in homozygous *rrm-1* and *rrm-2* *Arabidopsis* mutant lines (Figure 3C). *G2p*, *MOS1*, *OZF2*,



611 *HSP70-1*, and *MT2A* transcripts were quantified in 21-days-old leaves, a tissue with high *RRM* expression (**Figure 3C**, right panel). *AtTERT* transcripts were quantified in 7-days-old seedlings (**Figure 3C**, left panel), as there is a very low *AtTERT* transcription in *Arabidopsis* leaves (Ogrocka et al., 2012). *G2p* and *TERT* transcript levels were significantly higher in both *rrm* T-DNA insertion lines, suggesting a possible role of RRM in the regulation of these genes and/or the stability of the mRNAs encoded by these genes. *MOS1*, *OZF2*, *HSP70-1*, and *MT2A* transcripts levels were similar in mutant and wild-type plants.

622 Using GENEVESTIGATOR software, we identified 2102 genes putatively transcriptionally co-regulated with *RRM* and/or with at least one of its interacting partners TERT, G2P, MOS1, OZF2, HSP70-1, and MT2A, using the same conditions subset in a similar or opposite manner. A narrow subset of 137 genes showed overlapping co-regulation with at least two of these

667 genes. We observed that *RRM* and genes encoding its presumed interactors were co-regulated with numerous ribosomal protein genes. Interestingly, most ribosomal protein genes possess a telobox, a short regulatory motif over-represented in 5' regions of *Arabidopsis* genes with sequences identical to the repeat (AAACCCT)_n of plant telomeres (Regad et al., 1994). Telobox motifs are also found in promoters of genes involved in DNA replication (Tremousaygue et al., 1999; Wang et al., 2011). Because of a possible link between the cell cycle-dependent regulation of the expression of genes encoding ribosomal proteins and telomerase (Gaspin et al., 2010), we selected for transcription analysis a subset of identified co-regulated genes in addition to genes involved in DNA replication and translation-related genes with known telobox motifs (**Table 1**). Five genes showed a 2- to 4-fold increase of transcript levels in both mutant lines, and four genes displayed an increase in the homozygous *rrm-1* line only. Interestingly, none of the genes analyzed showed

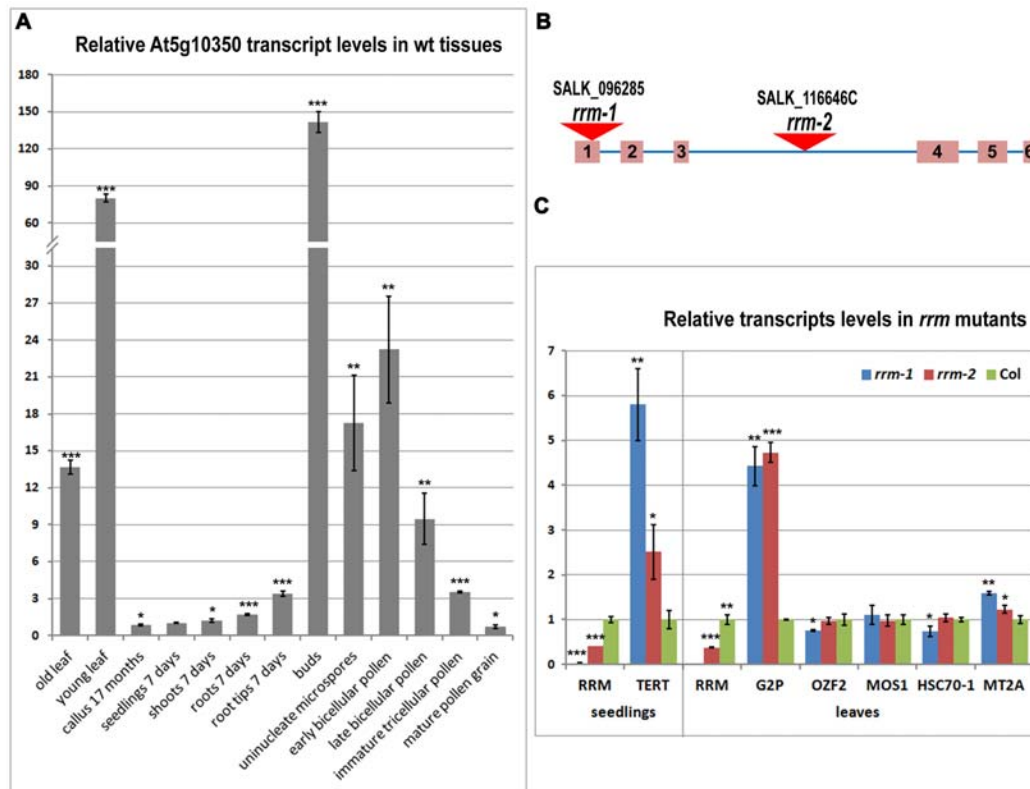


FIGURE 3 | Transcription profile of the RRM gene in tissues of wild-type plants and relative transcription of the RRM interactors in *rrm* mutants.

(A) Level of *RRM* transcripts in various wild-type (wt) plant tissues and developmental stages calculated relative to 7-days-old seedlings (Col-0) using the $\Delta\Delta Ct$ method and ubiquitin (*ubi10*) as a reference gene. (B) Schematic depiction of the *RRM* gene and position of the T-DNA insertion in homozygous mutant *Arabidopsis* lines *rrm-1* and *rrm-2*. (C) Level of transcripts of indicated genes in 7-days-old seedlings (left panel) and 21-days-old leaves (right panel) of *rrm-1* and *rrm-2* T-DNA insertion lines calculated relative to wild-type (Col-0) using the $\Delta\Delta Ct$ method and *ubi10* as a reference gene. Two-tailed *p*-values were calculated using the unpaired *t*-test (**p* < 0.05; ***p* < 0.001; ****p* = 0.0001, see Supplementary Table S2 for details).

significantly decreased transcript levels in the mutant lines. Transcript levels of DNA replication-related genes were not altered in either mutant line, suggesting that the telobox in the 5' region of these genes is not a critical determinant for RRM action.

DISCUSSION

The identification of RRM protein as a nuclear interactor with the CTE domain of AtTERT in tobacco BY2 protoplasts (Lee et al., 2012) was somehow surprising. However, yeast genome-wide screens (Askree et al., 2004; Gatbonton et al., 2006; Ungar et al., 2009) revealed a number of proteins that influenced telomere length and which were involved in numerous cellular processes without a known link to telomere maintenance. Among these were human proteins involved in RNA metabolism and transcription pathways connected with non-telomeric functions of telomerase (see Majerska et al., 2011 for review). Conserved protein structure comprising the coiled-coil N-terminus, a single internal RRM domain, and the C-terminal region with nuclear localization signal

classified the RRM protein as a nuclear poly(A) binding protein (PABPN, Eliseeva et al., 2013). Recently, a RRM protein was identified as an interactor with AtCSP3 (COLD SHOCK DOMAIN PROTEIN 3; Kim et al., 2013), and hnRNP-like proteins (Arabidopsis Interactome Mapping Consortium, et al., 2011). Here, we verified RRM interaction with the CTE domain of AtTERT using BiFC in *Arabidopsis* protoplasts, but their direct interaction was not observed in yeast. Known technical differences of both screening systems suggest that the *in vivo* interaction is mediated by an additional protein absent in the yeast cell, or it is facilitated by missing post-translational modifications. Analysis of T-DNA insertion mutant lines showed no obvious changes in telomere lengths and telomerase activity, suggesting that the RRM protein is not essential for telomere maintenance. The observed interaction with telomerase may reflect possible non-telomeric functions.

The localization of the RRM-YFP signal in nuclear speckles and the observation that all described BiFC RRM interactions (and interaction with CSP3 protein, Kim et al., 2013) are nuclear-localized suggest that RRM is in fact a PABPN. Human PABPN1 localizes to nuclear speckles as a consequence of

TABLE 1 | Relative transcription levels of genes with identified telobox sequences and/or co-regulated with RRM interactors in homozygous *rrm* mutants.

AGI number	Gene name	<i>rrm-1*</i>		<i>rrm-2*</i>		Telobox	Reference	Co-regulation with RRM and its interactors (GENEVESTIGATOR score) ^a
		2 ^{-ddCt}	SD	2 ^{-ddCt}	SD			
Genes encoding cytoplasmic ribosomal proteins								
At1g23290	RPL27a	2.08	0.37	2.56	1.23	Yes	In this work	RRM (0,73), G2P (0,89), HSP70-1 (0,78)
At1g72370	RP40	4.72	0.13	3.42	0.22	Yes	Tremousaygue et al., 1999; Manevski et al., 2000	RRM (0,75), G2P (0,92), HSP70-1 (0,77)
At3g04840	RPS3Ae family	1.78	0.10	1.34	0.11	Yes	In this work	RRM (0,78), G2P (0,89), HSP70-1 (0,76)
At3g25520	RPL5	1.66	0.07	1.32	0.11	Yes	In this work	RRM (0,84), G2P (0,90), HSP70-1 (0,84)
At5g39740	RPL5b	1.41	0.01	1.12	0.13	Yes	In this work	RRM (0,87), G2P (0,90), HSP70-1 (0,75)
At3g47370	RPS10p/S20e family	2.30	0.01	1.45	0.10	Yes	In this work	RRM (0,73), MOS1 (-0,81), G2P (0,90), HSP70-1 (0,73)
At3g49010	BBC1	3.70	0.55	1.86	0.24	Yes	In this work	RRM (0,83), G2P (0,92), HSP70-1 (0,77)
At3g51190	RPL2 family	2.41	0.2	1.89	0.11	Yes	In this work	n.a.
At3g56340	RPS26e family	1.38	0.03	1.17	0.08	Yes	In this work	RRM (0,75), HSP70-1 (0,68)
At3g60770	RPS13/S15 family	1.95	0.12	1.44	0.07	Yes	In this work	RRM (0,78), G2P (0,90), HSP70-1 (0,80)
At4g00810	RPS60 family	2.39	0.09	2.25	0.10	Yes	Tremousaygue et al., 1999	MOS1 (-0,88)
At4g09800	RPS18C	2.69	0.23	2.35	0.05	Yes	Tremousaygue et al., 1999	No co-regulation
Genes encoding plastid ribosomal proteins								
At1g79850	PRPS17	0.68	0.02	1.68	0.28	Yes	Tremousaygue et al., 1999	No co-regulation
At2g33450	PRPL28	2.62	0.55	1.33	0.15	Yes	Tremousaygue et al., 1999	No co-regulation
Genes encoding translation factors								
At1g07940	EF1A family	1.88	0.01	0.87	0.01	Yes	Tremousaygue et al., 1999	No co-regulation
At1g54290	TIF SUI1 family	2.77	0.23	2.43	0.34	Yes	Tremousaygue et al., 1999	No co-regulation
DNA replication-related genes								
At1g07270	CDC6b	0.98	0.11	1.03	0.08	No	In this work	No co-regulation
At1g07370	PCNA1	1.13	0.07	1.13	0.11	Yes	Manevski et al., 2000	No co-regulation
At1g44900	MCM2	0.97	0.13	0.99	0.12	Yes	In this work	No co-regulation
At5g46280	MCM3	0.68	0.02	0.95	0.08	Yes	In this work	No co-regulation
At2g16440	MCM4	0.94	0.01	0.94	0.06	No	In this work	No co-regulation
At2g07690	MCM5	0.95	0.07	0.99	0.08	No	In this work	No co-regulation
At5g44635	MCM6	0.72	0.03	0.90	0.12	Yes	In this work	n.a.
At4g02060	MCM7	1.03	0.07	0.97	0.13	Yes	In this work	No co-regulation
Other co-regulated genes								
At2g19480	NAP1;2	1.85	0.15	1.42	0.15	Yes	In this work	RRM (0,79), HSP70-1 (0,75)
At3g54230	SUA	1.54	0.22	1.25	0.09	Yes	In this work	TERT (0,88), MOS1 (0,95)
At4g17520	Hyaluronan family	0.60	0.21	1.55	0.13	Yes	In this work	RRM (0,77), G2P (0,93)
At5g14790	ARM superfamily	0.76	0.05	0.87	0.08	No	In this work	TERT (-0,84)

^an.a., data not available; *more than twofold change in transcript level (2^{-ddCt}) is highlighted; SD, standard deviation.

RNA poly(A) binding (Calado and Carmo-Fonseca, 2000). Our observations indicate a conserved structure-localization relation of PABPNs across eukaryotic species. Nucleic acid binding of RRM-containing proteins is often mediated by a pair of RRM

domains (Deo et al., 1999; Kwon and Chung, 2004). On the other hand, *Xenopus laevis* XlePABP2 and *Citrus sinensis* CsPABPN1, PABPNs that share similar structure with RRM protein, both bind poly(A) as monomers and undergo a dimer-monomer transition upon poly(A) binding (Song et al., 2008; Domingues et al., 2015). We visualized RRM protein dimerization in tobacco BY-2 protoplasts and observed the same nuclear speckle pattern as with RRM-YFP localization. Moreover, we demonstrated that RRM protein dimerizes through its C-terminal region. This last observation contradicts the published dimerization model of hPABPN1 (Ge et al., 2008), which identified the amino acid residues responsible for self-interaction within the RRM domain.

We revealed possible connection between RRM and non-canonical telomerase functions by identifying interaction partners of RRM. Screening for nYFP-RRM protein-protein interactions against a cYFP-tagged cDNA library identified five putative RRM interactors with various annotated functions such as transcription regulation (OZF2), epigenetic regulation (MOS1), mRNA catabolism (MOS1), RNA methylation (G2p), protein nuclear import (G2p), protein folding (HSP70-1), proteolysis (G2p), cellular copper ion homeostasis (MT2A), or metabolism (MOS1, HSP70-1). In all five cases, the interaction localization pattern resembles nuclear speckles, as observed for RRM-YFP subcellular localization. A G2p-GFP fusion protein was previously localized in the nucleus (Zhang et al., 2005). However, the subcellular localization of other RRM interactors has not previously been described. Interestingly, other data from our groups showed that G2p and MOS1 co-purify with TERT (Figure 2, Majerska et al., manuscript in preparation) and G2p and MT2A interact with TERT(RID1) using BiFC in tobacco BY-2 protoplasts (Figure 2B, Supplementary Figure S2), suggesting co-existence of TERT, RRM, G2p, MOS1, and MT2A in a multiprotein complex.

Analysis of telomere length and telomerase activity in homozygous *rrm-1* and *rrm-2* T-DNA insertion mutants indicated that the RRM protein was not important for the canonical telomeric functions of telomerase. On the other hand, *TERT* transcripts were elevated in homozygous *rrm* mutants, and TERT and RRM may share binding partners such as G2p, MOS1, and MT2A. These observations suggest that RRM plays a role in non-telomeric activities of telomerase. Interestingly, the G7 generation of a homozygous *tert* T-DNA insertion line showed increased *OZF2* and *MT2A* transcript levels (Amiard et al., 2014). PABPNs are implicated in processes that might be crucial for post-transcriptional regulation of gene expression. Our qPCR analyses indicated that RRM might generally function as a negative regulator of gene expression, because none of the 34 genes analyzed here showed significant decrease in transcript levels in homozygous *rrm* mutants. Increased levels of *TERT* and *G2p* transcripts in homozygous *rrm* mutant lines indicated a possible feedback mechanism in RRM-TERT and RRM-G2p interactions. Moreover, nine ribosomal and translation-related genes also showed significantly increased transcript levels in a *rrm* mutant background. We have further analyzed these nine genes for transcript level perturbations across different conditions using

GENEVESTIGATOR. *RPL2* transcripts were stable across various conditions. Interestingly, the transcript levels of the other eight genes changed more than twofold in response to salt stress in the *myb44* T-DNA insertion line (Jung et al., 2008). RP40, RPL27A, RPS10p/S20e, BBC1, and RPL2 form a protein interaction network (STRING database¹⁶, Szklarczyk et al., 2015) and are mutually co-regulated. The RRM interactome, subcellular localization, and co-regulation profile showing that the expression of the majority of its co-regulated genes contain telobox motifs in their promoters, further support the hypothesis that RRM may function in mediating non-telomeric (non-canonical) functions of telomerase. DNA replication-related genes were not co-regulated with genes encoding RRM or its interactors, and they also did not show changes in transcript abundance in a homozygous *rrm* background. These results suggest that the telobox in promoters of these genes are not a critical determinant of RRM action. Regulation of translation-related genes is generally important for the regulation of protein synthesis and consequently for cell growth. These genes regulate tumor onset and progression (reviewed in Loreni et al., 2014), further indicating a possible link between RRM and its interactors to TERT non-telomeric functions. Our results support a functional connection between RRM and its interaction partners in plant regulatory protein complex(es).

CONCLUSION

The RRM protein was previously identified as an interaction partner of AtTERT. However, telomere length shortening in knockout mutant plants was not significant. By screening a cDNA library using cYFP-RRM as a bait, we identified five interaction partners; two of them interacted also with TERT fragments. Investigation of the subcellular localization and protein structure suggested that RRM-protein may function as a nuclear poly(A)-binding protein. Transcriptional profiling revealed a possible involvement of RRM-protein in the regulation of a subset of ribosomal and translation-related genes. Most of these genes contain a telobox motif in their promoters. *G2p* and *TERT* transcript levels were significantly higher in *rrm/-* knockout mutants, suggesting a possible role for RRM in the regulation of these genes and/or the stability of the mRNAs encoded by these genes. Overlaps of the RRM and TERT interactome, subcellular localization of protein-protein interactions, and co-regulation profiles support the hypothesis that RRM may be involved in mediating non-canonical telomerase functions.

AUTHOR CONTRIBUTION

LD performed most of experiments except pollen RT-qPCR performed by DH and RR. LL was involved in cDNA screening, ES was involved in cloning. ES and SG designed the study.

¹⁶<http://www.string-db.org/>

1027 **FUNDING**

1028
1029 The work was supported by Czech Ministry of Education,
1030 Youth and Sports (project Interaktom, LH10352), the
1031 Grant Agency of the Czech Republic (13-06943S) and
1032 by the project “CEITEC – Central European Institute of
1033 Technology” (CZ.1.05/1.1.00/02.0068) from the European
1034 Regional Development Fund. Work in the Gelvin laboratory

1035
1036
1037 **REFERENCES**

1038 Amiard, S., Da Ines, O., Gallego, M. E., and White, C. I. (2014).
1039 Responses to telomere erosion in plants. *PLoS ONE* 9:e86220. doi:
1040 10.1371/journal.pone.0086220
1041 Arabidopsis Interactome Mapping Consortium, Dreze, M., Carvunis, A.,
1042 Charleateaux, B., Galli, M., Pevzner, S., et al. (2011). Evidence for network
1043 evolution in an *Arabidopsis* interactome map. *Science* 333, 601–607. doi:
1044 10.1126/science.1203877
1045 Askree, S. H., Yehuda, T., Smolikov, S., Gurevich, R., Hawk, J., Coker, C., et al.
1046 (2004). A genome-wide screen for *Saccharomyces cerevisiae* deletion mutants
1047 that affect telomere length. *Proc. Natl. Acad. Sci. U.S.A.* 101, 8658–8663. doi:
1048 10.1073/pnas.0401263101
1049 Blasco, M. A. (2005). Mice with bad ends: mouse models for the study of
1050 telomeres and telomerase in cancer and aging. *EMBO J.* 24, 1095–1103. doi:
1051 10.1038/sj.emboj.7600598
1052 Calado, A., and Carmo-Fonseca, M. (2000). Localization of poly(A)-binding
1053 protein 2 (PABP2) in nuclear speckles is independent of import into the nucleus
1054 and requires binding to poly(A) RNA. *J. Cell Sci.* 113(Pt 12), 2309–2318.
1055 Citovsky, V., Lee, L. Y., Vyas, S., Glick, E., Chen, M. H., Vainstein, A.,
1056 et al. (2006). Subcellular localization of interacting proteins by bimolecular
1057 fluorescence complementation in planta. *J. Mol. Biol.* 362, 1120–1131. doi:
1058 10.1016/j.jmb.2006.08.017
1059 Counter, C. M., Avilion, A. A., Lefeuvre, C. E., Stewart, N. G., Greider, C. W.,
1060 Harley, C. B., et al. (1992). Telomere shortening associated with chromosome
1061 instability is arrested in immortal cells which express telomerase activity.
1062 *EMBO J.* 11, 1921–1929.
1063 Deo, R. C., Bonanno, J. B., Sonenberg, N., and Burley, S. K. (1999). Recognition
1064 of polyadenylate RNA by the poly(A)-binding protein. *Cell* 98, 835–845. doi:
1065 10.1016/S0092-8674(00)81517-2
1066 Domingues, M. N., Sforca, M. L., Soprano, A. S., Lee, J., De Souza Tde, A.,
1067 Cassago, A., et al. (2015). Structure and mechanism of dimer-monomer
1068 transition of a plant poly(A)-binding protein upon RNA interaction:
1069 insights into its poly(A) tail assembly. *J. Mol. Biol.* 427, 2491–2506. doi:
1070 10.1016/j.jmb.2015.05.017
1071 Eliseeva, I. A., Lyabin, D. N., and Ovchinnikov, L. P. (2013). Poly(A)-
1072 binding proteins: structure, domain organization, and activity
1073 regulation. *Biochemistry Mosc.* 78, 1377–1391. doi: 10.1134/S00062979131
1074 30014
1075 Fitzgerald, M. S., Mcknight, T. D., and Shippen, D. E. (1996). Characterization and
1076 developmental patterns of telomerase expression in plants. *Proc. Natl. Acad. Sci.*
1077 *U.S.A.* 93, 14422–14427. doi: 10.1073/pnas.93.25.14422
1078 Fojtová, M., Peska, V., Dobsakova, Z., Mozgova, I., Fajkus, J., and Sykorova, E.
1079 (2011). Molecular analysis of T-DNA insertion mutants identified putative
1080 regulatory elements in the ATERT gene. *J. Exp. Bot.* 62, 5531–5545. doi:
1081 10.1093/jxb/err235
1082 Gaspin, C., Rami, J. F., and Lescure, B. (2010). Distribution of short interstitial
1083 telomere motifs in two plant genomes: putative origin and function. *BMC Plant*
1084 *Biol.* 10:283. doi: 10.1186/1471-2229-10-283
1085 Gathbonton, T., Imbisi, M., Nelson, M., Akey, J. M., Ruderfer, D. M., Kruglyak, L.,
1086 et al. (2006). Telomere length as a quantitative trait: genome-wide survey and
1087 genetic mapping of telomere length-control genes in yeast. *PLoS Genet.* 2:e35.
1088 doi: 10.1371/journal.pgen.0020035
1089 Ge, H., Zhou, D., Tong, S., Gao, Y., Teng, M., and Niu, L. (2008). Crystal structure
1090 and possible dimerization of the single RRM of human PABPN1. *Proteins* 71,
1091 1539–1545. doi: 10.1002/prot.21973

1084 is supported by grants from the US National Science
1085 Foundation.

1086
1087 **SUPPLEMENTARY MATERIAL**

1088
1089 The Supplementary Material for this article can be found online
1090 at: <http://journal.frontiersin.org/article/10.3389/fpls.2015.00985>

1091 **Q10**
1092
1093 Gohring, J., Fulcher, N., Jacak, J., and Riha, K. (2014). TeloTool: a new tool
1094 for telomere length measurement from terminal restriction fragment analysis
1095 with improved probe intensity correction. *Nucleic Acids Res.* 42:e21. doi:
1096 10.1093/nar/gkt1315
1097 Greider, C. W., and Blackburn, E. H. (1985). Identification of a specific telomere
1098 terminal transferase activity in *Tetrahymena* extracts. *Cell* 43, 405–413. doi:
1099 10.1016/0092-8674(85)90170-9
1100 Greider, C. W., and Blackburn, E. H. (1987). The telomere terminal transferase
1101 of *Tetrahymena* is a ribonucleoprotein enzyme with two kinds of primer
1102 specificity. *Cell* 51, 887–898. doi: 10.1016/0092-8674(87)90576-9
1103 Harley, C. B., Futcher, A. B., and Greider, C. W. (1990). Telomeres shorten
1104 during ageing of human fibroblasts. *Nature* 345, 458–460. doi: 10.1038/345
1105 458a0
1106 Hruz, T., Laule, O., Sza bo, G., Wessendorp, F., Bleuler, S., Oertle, L., et al. (2008).
1107 Genevestigator v3: a reference expression database for the meta-analysis of
1108 transcriptomes. *Adv. Bioinformatics* doi: 10.1155/2008/420747
1109 Jung, C., Seo, J. S., Han, S. W., Koo, Y. J., Kim, C. H., Song, S. I., et al. (2008).
1110 Overexpression of AtMYB44 enhances stomatal closure to confer abiotic
1111 stress tolerance in transgenic *Arabidopsis*. *Plant Physiol.* 146, 623–635. doi:
1112 10.1104/pp.107.110981
1113 Keller, R. W., Kuhn, U., Aragon, M., Bornikova, L., Wahle, E., and Bear, D. G.
1114 (2000). The nuclear poly(A) binding protein, PABP2, forms an oligomeric
1115 particle covering the length of the poly(A) tail. *J. Mol. Biol.* 297, 569–583. doi:
1116 10.1006/jmbi.2000.3572
1117 Kim, M. H., Sonoda, Y., Sasaki, K., Kaminaka, H., and Imai, R. (2013). Interactome
1118 analysis reveals versatile functions of *Arabidopsis* COLD SHOCK DOMAIN
1119 PROTEIN 3 in RNA processing within the nucleus and cytoplasm. *Cell Stress*
1120 *Chaperones* 18, 517–525. doi: 10.1007/s12192-012-0398-3
1121 Krietsch, J., Rouleau, M., Pic, E., Ethier, C., Dawson, T. M., Dawson, V. L., et al.
1122 (2013). Reprogramming cellular events by poly(ADP-ribose)-binding proteins.
1123 *Mol. Aspects Med.* 34, 1066–1087. doi: 10.1016/j.mam.2012.12.005
1124 Kuhn, U., Gundel, M., Knoth, A., Kerwitz, Y., Rudel, S., and Wahle, E. (2009).
1125 Poly(A) tail length is controlled by the nuclear poly(A)-binding protein
1126 regulating the interaction between poly(A) polymerase and the cleavage
1127 and polyadenylation specificity factor. *J. Biol. Chem.* 284, 22803–22814. doi:
1128 10.1074/jbc.M109.018226
1129 Kwon, C., and Chung, I. K. (2004). Interaction of an *Arabidopsis* RNA-binding
1130 protein with plant single-stranded telomeric DNA modulates telomerase
1131 activity. *J. Biol. Chem.* 279, 12812–12818. doi: 10.1074/jbc.M312011200
1132 Lee, L. Y., Wu, F. H., Hsu, C. T., Shen, S. C., Yeh, H. Y., Liao, D. C., et al. (2012).
1133 Screening a cDNA library for protein-protein interactions directly in planta.
1134 *Plant Cell* 24, 1746–1759. doi: 10.1105/tpc.112.097998
1135 Levy, M. Z., Allsopp, R. C., Futcher, A. B., Greider, C. W., and Harley, C. B. (1992).
1136 Telomere end-replication problem and cell aging. *J. Mol. Biol.* 225, 951–960.
1137 doi: 10.1016/0022-2836(92)90096-3
1138 Loreni, F., Mancino, M., and Biffo, S. (2014). Translation factors and ribosomal
1139 proteins control tumor onset and progression: how? *Oncogene* 33, 2145–2156.
1140 doi: 10.1038/onc.2013.153
1141 Lorkovic, Z. J., Hilscher, J., and Barta, A. (2004). Use of fluorescent protein
1142 tags to study nuclear organization of the spliceosomal machinery in
1143 transiently transformed living plant cells. *Mol. Biol. Cell* 15, 3233–3243. doi:
1144 10.1091/mbc.E04-01-0055
1145 Majerska, J., Sykorova, E., and Fajkus, J. (2011). Non-telomeric activities of
1146 telomerase. *Mol. Biosyst.* 7, 1013–1023. doi: 10.1039/c0mb00268b
1147 Manevski, A., Bertoni, G., Bardet, C., Tremousaygue, D., and Lescure, B. (2000).
1148 In synergy with various cis-acting elements, plant interstitial telomere motifs
1149

- 1141 regulate gene expression in *Arabidopsis* root meristems. *FEBS Lett.* 483, 43–46. doi: 10.1016/S0014-5793(00)02056-1
- 1142
- 1143 Ogrocka, A., Sykorova, E., Fajkus, J., and Fojtova, M. (2012). Developmental silencing of the AtTERT gene is associated with increased H3K27me3 loading and maintenance of its euchromatic environment. *J. Exp. Bot.* 63, 4233–4241. doi: 10.1093/jxb/ers107
- 1144
- 1145
- 1146 Olovnikov, A. M. (1971). [Principle of marginotomy in template synthesis of polynucleotides]. *Dokl. Akad. Nauk. SSSR* 201, 1496–1499.
- 1147
- 1148 Olovnikov, A. M. (1973). A theory of marginotomy. The incomplete copying of template margin in enzymic synthesis of polynucleotides and biological significance of the phenomenon. *J. Theor. Biol.* 41, 181–190. doi: 10.1016/0022-5193(73)90198-7
- 1149
- 1150
- 1151 Pfaffl, M. W. (2004). “Quantification strategies in real-time PCR,” in *A-Z of Quantitative PCR*, ed. S. A. Bustin (La Jolla, CA: International University Line), 87–112.
- 1152
- 1153 Regad, F., Lebas, M., and Lescure, B. (1994). Interstitial telomeric repeats within the *Arabidopsis thaliana* genome. *J. Mol. Biol.* 239, 163–169. doi: 10.1006/jmbi.1994.1360
- 1154
- 1155
- 1156 Schruppová, P. P., Vychodilova, I., Dvorackova, M., Majerska, J., Dokladal, L., Schorova, S., et al. (2014). Telomere repeat binding proteins are functional components of *Arabidopsis* telomeres and interact with telomerase. *Plant J.* 77, 770–781. doi: 10.1111/tpj.12428
- 1157
- 1158
- 1159 Seimiya, H., Sawada, H., Muramatsu, Y., Shimizu, M., Ohko, K., Yamane, K., et al. (2000). Involvement of 14-3-3 proteins in nuclear localization of telomerase. *EMBO J.* 19, 2652–2661. doi: 10.1093/emboj/19.11.2652
- 1160
- 1161
- 1162 Song, J., McGivern, J. V., Nichols, K. W., Markley, J. L., and Sheets, M. D. (2008). Structural basis for RNA recognition by a type II poly(A)-binding protein. *Proc. Natl. Acad. Sci. U.S.A.* 105, 15317–15322. doi: 10.1073/pnas.0801274105
- 1163
- 1164 Sykorova, E., and Fajkus, J. (2009). Structure-function relationships in telomerase genes. *Biol. Cell* 101, 375–392. doi: 10.1042/BC20080205
- 1165
- 1166 Szklarczyk, D., Franceschini, A., Wyder, S., Forslund, K., Heller, D., Huerta-Cepas, J., et al. (2015). STRING v10: protein-protein interaction networks, integrated over the tree of life. *Nucleic Acids Res.* 43, D447–D452. doi: 10.1093/nar/gku1003
- 1167
- 1168
- 1169 Tenea, G. N., Spantzel, J., Lee, L. Y., Zhu, Y., Lin, K., Johnson, S. J., et al. (2009). Overexpression of several *Arabidopsis* histone genes increases Agrobacterium-mediated transformation and transgene expression in plants. *Plant Cell* 21, 3350–3367. doi: 10.1105/tpc.109.070607
- 1170
- 1171
- 1172
- 1173
- 1174
- 1175
- 1176
- 1177
- 1178
- 1179
- 1180
- 1181
- 1182
- 1183
- 1184
- 1185
- 1186
- 1187
- 1188
- 1189
- 1190
- 1191
- 1192
- 1193
- 1194
- 1195
- 1196
- 1197
- Tremousaygue, D., Manevski, A., Bardet, C., Lescure, N., and Lescure, B. (1999). Plant interstitial telomere motifs participate in the control of gene expression in root meristems. *Plant J.* 20, 553–561. doi: 10.1046/j.1365-313X.1999.00627.x
- 1198
- 1199
- 1200
- 1201 Ungar, L., Yosef, N., Sela, Y., Sharan, R., Ruppin, E., and Kupiec, M. (2009). A genome-wide screen for essential yeast genes that affect telomere length maintenance. *Nucleic Acids Res.* 37, 3840–3849. doi: 10.1093/nar/gkp259
- 1202
- 1203
- 1204 Wahle, E., and Rueggsegger, U. (1999). 3'-End processing of pre-mRNA in eukaryotes. *FEMS Microbiol. Rev.* 23, 277–295. doi: 10.1016/S0168-6445(99)00008-X
- 1205
- 1206
- 1207 Wang, J., Wang, Y., Wang, Z., Liu, L., Zhu, X. G., and Ma, X. (2011). Synchronization of cytoplasmic and transferred mitochondrial ribosomal protein gene expression in land plants is linked to Telo-box motif enrichment. *BMC Evol. Biol.* 11:161. doi: 10.1186/1471-2148-11-161
- 1208
- 1209
- 1210 Watson, J. D. (1972). Origin of concatemeric T7 DNA. *Nat. New Biol.* 239, 197–201. doi: 10.1038/newbio239197a0
- 1211
- 1212 Wu, F. H., Shen, S. C., Lee, L. Y., Lee, S. H., Chan, M. T., and Lin, C. S. (2009). Tape-*Arabidopsis* sandwich - a simpler *Arabidopsis* protoplast isolation method. *Plant Methods* 5:16. doi: 10.1186/1746-4811-5-16
- 1213
- 1214 Zachova, D., Fojtova, M., Dvorackova, M., Mozgova, I., Lermontova, I., Peska, V., et al. (2013). Structure-function relationships during transgenic telomerase expression in *Arabidopsis*. *Physiol. Plant* 149, 114–126. doi: 10.1111/ppl.12021
- 1215
- 1216
- 1217 Zhang, W. K., Shen, Y. G., He, X. J., Du, B. X., Xie, Z. M., Luo, G. Z., et al. (2005). Characterization of a novel cell cycle-related gene from *Arabidopsis*. *J. Exp. Bot.* 56, 807–816. doi: 10.1093/jxb/eri075
- 1218
- 1219
- 1220
- 1221
- 1222
- 1223
- 1224
- 1225
- 1226
- 1227
- 1228
- 1229
- 1230
- 1231
- 1232
- 1233
- 1234
- 1235
- 1236
- 1237
- 1238
- 1239
- 1240
- 1241
- 1242
- 1243
- 1244
- 1245
- 1246
- 1247
- 1248
- 1249
- 1250
- 1251
- 1252
- 1253
- 1254
- 1255
- Conflict of Interest Statement:** The authors declare that the research was conducted in the absence of any commercial or financial relationships that could be construed as a potential conflict of interest.
- Copyright © 2015 Dokládal, Honys, Rana, Lee, Gelvin and Sykorová. This is an open-access article distributed under the terms of the Creative Commons Attribution License (CC BY). The use, distribution or reproduction in other forums is permitted, provided the original author(s) or licensor are credited and that the original publication in this journal is cited, in accordance with accepted academic practice. No use, distribution or reproduction is permitted which does not comply with these terms.*